NeuroImage 196 (2019) 318–328

Contents lists available at ScienceDirect

NeuroImage

journal homepage: www.elsevier.com/locate/neuroimage

The relationship between heart rate and functional connectivity of brain regions involved in autonomic control

Feliberto de la Cruz [a], Andy Schumann [a], Stefanie Köhler [a], Jürgen R. Reichenbach [b,c], Gerd Wagner [a], Karl-Jürgen Bär [a,*]

[a] Psychiatric Brain and Body Research Group, Department of Psychiatry and Psychotherapy, Jena University Hospital, Jena, Germany
[b] Medical Physics Group, Department of Diagnostic and Interventional Radiology, Jena University Hospital, Jena, Germany
[c] Michael Stifel Center for Data-driven and Simulation Science Jena, Friedrich Schiller University, Jena, Germany

A B S T R A C T

The peripheral autonomic nervous system (ANS) adjusts the heart rate (HR) to intrinsic and extrinsic demands. It is controlled by a group of functionally connected brain regions assembling the so-called central autonomic network (CAN). More specifically, forebrain cortical regions, limbic and brainstem structures within the CAN have been identified as important components of circuits involved in HR regulation. The present study aimed to investigate whether functional connectivity (FC) between these regions varies in subjects with different heart rates. Thus, 84 healthy subjects were separated according to their HR in slow, medium and fast. We observed a direct association between HR and FC in CAN regions, where stronger FC was related to slower HR. This relationship, however, is non-linear, follows an exponential course and is not restricted to CAN areas only. The network-based analysis (NBS) using time series from 262 independent anatomical ROIs revealed significantly increased functional connectivity in subjects with slow HR compared to subjects with fast HR mainly in regions being part of the salience network, but also of the default-mode network. We additionally simulated the effect of aliasing on the functional connectivity using several TRs and heart rates to exclude the possibility that FC differences might be due to different aliasing effects in the data. The result of the simulation indicated that aliasing cannot explain our findings.

Thus, present results imply a functionally meaningful coupling between FC and HR that need to be accounted for in future studies. Moreover, given the established link between HR and emotional, cognitive and social processes, present findings may also be considered to explain individual differences in brain activation or connectivity when using corresponding paradigms in the MR scanner to investigate such processes.

1. Introduction

The activity of the heart, despite being equipped with intrinsic automaticity, is influenced by almost all the other organs of the body. Body signals shape the workload of the heart in order to meet changing needs of the entire organism. The two peripheral branches of the ANS, the parasympathetic and the sympathetic system, modulate the intrinsic activity of the cardiac pacemaker cells in the sinoatrial node. While the parasympathetic or vagal activity reducing energy expenditure is anabolic and health promoting, the sympathetic branch is needed for an adequate stress response. Thus, the heart rate and its variability mirror the resulting homeostasis of an organism influenced by physical as well as by psychological variables in a certain environment. It is therefore conceivable that a complex system is needed to orchestrate the autonomic function of the body to meet all internal and external needs. Based on animal experiments, Benarroch coined the term “central autonomic network” (CAN) in 1993 in order to describe a group of forebrain, limbic and brainstem regions involved in the generation of an adequate autonomic functional state (Benarroch, 1993).

In 2000, Thayer and colleagues developed the Neurovisceral Integration Model to provide a theoretical framework linking cardiac regulation through activation of the CAN to cognitive and emotional states. It comprises not only central autonomic nuclei within the brainstem or limbic structures, i.e. insula or amygdala, but moreover also cortico-limbic structures including the cingulate cortex and the ventromedial prefrontal cortex (VMPFC) (Thayer and Lane, 2000).

These brain regions, especially the VMPFC, exerts top-down control on the responses of subcortical structures, i.e. cingulate and anterior insular cortices together with the amygdala, which form an interconnected network and modulate the activity of subcortical/brainstem downstream regions, i.e. periaqueductal gray, hypothalamus and brainstem nuclei. These latter regions, in turn, finalize the autonomic output to the body by modulating the parasympathetic/sympathetic balance.

In support of this model, we identified in a previous meta-analysis of various neuroimaging studies on central regulation of the ANS, anterior (ACC) and midcingulate cortices (MCC), anterior insula (aI), VMPFC,

* Corresponding author. Department of Psychiatry and Psychotherapy, Jena University Hospital, Philosophenweg 3, 07743, Jena, Germany.
E-mail address: Karl-Juergen.Baer@med.uni-jena.de (K.-J. Bär).

https://doi.org/10.1016/j.neuroimage.2019.04.014
Received 25 January 2019; Received in revised form 27 March 2019; Accepted 3 April 2019
Available online 11 April 2019

mediodorsal thalamus, amygdala, hippocampus, and hypothalamus as central brain areas involved in ANS control (Beissner et al., 2013). This meta-analysis also revealed that sympathetic regulation mainly involves the prefrontal cortex, the ACC and MCC, the posterior insula, whereas parasympathetic regulation comprises rather the posterior cingulate (PCC) and lateral temporal cortices, and the hippocampus. AI and amygdala seem to be involved in both vagal and sympathetic control of autonomic function. Similarly, Shoemaker et al. (2015) described in their review on neural correlates of cardiovascular responses to exercise a cortico-limbic network, including VMPFC, dorsal ACC (dACC), amygdala, insula, and the hippocampus. In the meta-analysis by Thayer et al. (2012), the authors established a link between mainly amygdala and VMPFC activation during several cognitive as well as affective paradigms and the heart rate or its changes in variability (HRV). Taken together, all these functional neuroimaging studies provide a convincing basis that neural activity in the cortico-limbic regions is associated with autonomic cardiovascular regulation.

Analysis of functional connectivity (FC) of resting-state functional Magnetic Resonance Imaging (rs-fMRI) datasets is an established, powerful means to reveal the FC of a specific brain region or the network architecture (Biswal et al., 1995; Greicius et al., 2003). In this context, FC may help to uncover valuable information about brain correlates underlying heart rate regulation (Kumral et al., 2018; Sakaki et al., 2016). However, when studying the relationship between physiological measures such as heart rate and the fMRI signal, it is important to properly correct the fMRI data time series with respect to physiological noise. For instance, cardiac processes affect both the pulsation of blood and cerebrospinal fluid (CSF), which may result in artifacts near ventricles, sulci, and large vessels (Dagli et al., 1999; Glover et al., 2000). There is also growing evidence that fluctuations in the functions of the ANS, i.e. respiration and HR, strongly covary with the BOLD signal (Birn et al., 2006; Bright and Murphy, 2015; Chang et al., 2013; Iacovella and Hasson, 2011; Lund et al., 2006). Thus, it is important to separate physiological noise in form of respiratory and cardiac-rate related fluctuations from the neuronal-activity-related fluctuations associated with the ANS. Furthermore, undesired effects regarding differences in functional connectivity between groups with varying heart rates may occur, when using sampling rates determined by the repetition time (TR) of the MR imaging sequence that are lower than the Nyqvist frequency of the physiological signal. In such cases, the cardiac signal could alias into the low-frequency BOLD range and thus impact functional connectivity (Bhattacharyya and Lowe, 2004; Lowe, 1999; Tong et al., 2011).

Based on previous studies linking heart rate to CAN activity (Beissner et al., 2013; Thayer et al., 2012; Thayer and Lane, 2009, 2000), there is strong evidence to assume that different heart rates can be associated with changes in the functional coupling between CAN regions. Thus, the main goal of the present study was to investigate whether healthy young subjects, who were divided into groups according to their heart rate, exhibit differences in the resting state functional connectivity (RSFC) pattern between specific regions of the CAN. In the first step, we applied a region-of-interest (ROI) approach, focusing on differences between groups in whole brain RSFC, while using cortico-limbic ROIs of the CAN, i.e. amygdala, aI, and VMPFC, as seed regions. We selected these three regions as seed regions because, as mentioned before, amygdala and aI have been showed to be simultaneously involved in both vagal and sympathetic control, and therefore are essential for heart rate regulation. VMPFC, on the other hand, exerts top-down control on these subcortical structures and accompanying behavioral and physiological responses (Thayer et al., 2012).

Furthermore, previous studies indicated the central role of selected ROIs in emotion regulation or self-control (Mather and Thayer, 2018), serving as common units for regulating cardiac and affective states.

In the second step, and to circumvent some limitations associated with an ROI-based approach, we applied a recently developed statistical method called network-based statistic (NBS) to examine potential group differences in the whole brain network connectivity (Zalesky et al., 2010). Due to the central role of the insula and the amygdala within the brain's salience network (Menon, 2015) and of the VMPFC within the so-called default mode network (Buckner et al., 2008), we additionally expected to find differences in the FC within these networks related to differences in heart rate. Finally, since fMRI data were acquired with a standard TR of 2.5s, we additionally examined potential confounding effects caused by aliasing using simulated cardiac and fMRI signals at different heart rates and sampling frequencies.

2. Methods

2.1. Participants

84 healthy young subjects recruited from the local university community participated in the present study (age mean (M) = 31.58 yrs, SD = 10.76 yrs, 43 females). We formed three groups, each comprising 28 individuals, based on the mean heart rate as assessed by the MR scanner. The first group was restricted to HR < 60 bpm (M = 54.74 bpm, SD = 3.93 bpm) and referred here as “SLOW-HR” (SHR). The second group was defined by the range 60 bpm < HR < 75 bpm (M = 66.87 bpm, SD = 3.51 bpm) and called “MEDIUM-HR” (MHR). Finally, we defined a “FAST-HR” (FHR) group with HR > 75bpm (M = 81.21 bpm, SD = 6.21 bpm). The groups did not significantly differ regarding age or gender.

Informed written consent was obtained in accordance with the protocols approved by the local Ethics Committee and all subjects received an allowance of 10 Euro in return for their participation.

2.2. fMRI data acquisition

The data were collected on a 3T whole body system equipped with a 12-element head matrix coil (MAGNETOM TIM Trio, Siemens). The whole measurement consisted of a resting state scan followed by a high-resolution anatomical scan. Participants were instructed to keep their eyes closed during the whole measurement and to move as little as possible. T2*- weighted images were obtained using a gradient-echo EPI sequence accelerated by parallel imaging using GRAPPA (TR = 2520 ms, TE = 30 ms, FA = 90°, inter-slice gap = 0.625 mm, GRAPPA factor = 2) with 45 contiguous transverse slices of 2.5 mm thickness covering the entire brain and including the lower brainstem. The matrix size was 88 × 84 pixels with an in-plane resolution of 2.5 × 2.5 mm^2. A series of 240 whole-brain volume sets was acquired in one session. High-resolution anatomical T1-weighted volume scans (MPRAGE) were obtained in sagittal slice orientation (TR = 2300 ms, TE = 3.03 ms, TI = 900 ms, FA = 9°, acquisition matrix = 256 × 256 x 192, acceleration factor PAT = 2) with an isotropic resolution of 1 mm^3.

2.3. Physiological recordings and analyses

During the fMRI data acquisition, respiratory and cardiac signals (PPG) were simultaneously recorded using an MR-compatible BIOPAC MP150 polygraph (BIOPAC Systems Inc., Goleta, CA, USA) and digitized at 500 Hz. Respiratory activity was assessed by a strain gauge transducer incorporated in a belt tied around the chest, approximately at the level of the processus xiphoideus. The optical pulse sensor was attached to the proximal phalanx of the index finger of the subject's left hand. Each PPG recording was inspected for potential errors in the automatic PPG pulse detection routine. For instance, some movement artifacts might be erroneously identified as pulse waves. These errors were manually corrected by an expert (A.S.), who has longstanding experiences with preprocessing of physiological data. On average, less than 2% of the PPG pulses per subject were manually corrected. Inter-beat-interval (IBI) time series, based on the RR intervals, were derived from the PPG signal. Finally, mean subject's HR was computed as the inverse of the average IBI series and scaled to the unit beats-per-minute.

Skin conductance was measured continuously (constant voltage technique) at the left hand's palm with Ag/AgCl electrodes placed at the

thenar and hypothenar eminence. The signal was amplified below 10 Hz, median filtered (150 samples) and temporally smoothed (250 samples) to reduce the influence of noise. Skin conductance changes are mainly dependent on the activity of sweat glands innervated by the sympathetic system and can be used to index sympathetic arousal (Bach et al., 2010). *As shown by previous studies (*Deco et al., 2014; Patterson et al., 2002; Tagliazucchi and Laufs, 2014), changes in arousal may modulate neuronal activity in several brain areas and should be especially considered during the passive resting state investigation. The BOLD signal variability due to differences in the arousal may further confound the significance of the studied functional networks. Thus, we assessed sympathetic skin responses to control for the arousal level of all participants (Bach et al., 2010). We estimated the overall level of the skin conductance (SLC) by averaging the skin conductance signal. Spontaneous skin conductance fluctuations (SCF) were identified by a pattern matching algorithm using the characteristic shape of an SCF described mathematically by Lim and colleagues (Lim et al., 1997). This approach is robust in the presence of noise and less dependent on the individual electrode contact resistance than other threshold-based approaches (Boucsein, 1992; Lim et al., 1997).

2.4. Resting state fMRI preprocessing

Data preprocessing was performed using AFNI (https://afni.nimh.nih.gov/) and SPM12 (http://www.fil.ion.ucl.ac.uk/spm). The first five images were discarded allowing magnetization to reach a steady state. Prior to preprocessing, a state-of-the-art physiological noise correction was carried out. The model included four regressors to reduce artifacts synchronized with the respiratory cycle (Glover et al., 2000) and five respiration volumes per time (RVT) regressors that model slow blood oxygenation level fluctuations (Birn et al., 2008; Chang et al., 2009). The RVT regressors consisted of the RVT function and four delayed terms at 5, 10, 15, and 20 s (Birn et al., 2008). All regressors were generated on a slice-wise basis by AFNI's RetroTS.m script (Jo et al., 2010).

Further preprocessing included slice timing correction with Fourier interpolation and realignment to the first EPI volume using a rigid body transformation. It was ensured that head movement was below 3 mm and 3° for each participant. Additional preprocessing steps were (i) removal of linear and quadratic trends and of several sources of variance, i.e., head-motion parameters, CSF and white matter signal, (ii) temporal band-pass filtering, retaining frequencies in the 0.01–0.1 Hz band, and (iii) spatial smoothing using a Gaussian kernel of full-width half maximum of 6 mm. An optimized cardiac response function (CRF) with respect to the subject's HR (de la Cruz et al., 2017) was additionally included as a nuisance covariate to model low-frequency HR fluctuations. Extra-cerebral tissue was removed from the anatomical images using ROBEX (Iglesias et al., 2011), a learning-based brain extraction method trained on manually "skull-stripped" data from healthy subjects. These skull-stripped brains were aligned to the standard MNI 2-mm brain. Finally, functional images were registered to anatomical data and normalized to the MNI space by applying transformation parameters derived from the anatomical to MNI registration.

2.5. Regions of interest and functional connectivity analyses

Based on our hypothesis, five ROIs - one in the VMPFC, one in each hemisphere of the aI and one in each hemisphere of the amygdala - were defined as seed regions for the functional connectivity analyses. The VMPFC-ROI was drawn as a sphere of 10 mm radius, centered at MNI-coordinates, $x = 0$, $y = 44$, $z = -14$, as defined in our previous study (Bär et al., 2016). Anterior insula and amygdala ROIs were created using the WFU Pick Atlas tool for SPM (Maldjian et al., 2004, 2003). The aI was defined as the most anterior part starting from $y \geq 6$ mm along the posterior-anterior axis, which is in accordance with previous literature (Cauda et al., 2012, 2011). We divided the whole insula ROI based on the WFU Pick Atlas into two sub-regions using a perpendicular plane that cuts the posterior-anterior axis at $y = 6$. Only the anterior section was used in the analyses.

To obtain functional connectivity maps, the preprocessed resting-state fMRI signal was averaged over each seed region and correlated against all voxels in the brain. The resulting Pearson correlation coefficients were converted to Fisher z statistic in order to produce a more normally distributed variable (Zar, 1996). Comparison of functional connectivity maps between SHR, MHR and FHR groups was then performed using a one-way analysis of variance (ANOVA). The overall main effect of group (F-test) for each seed regions was thresholded at $p < 0.001$ and corrected for multiple comparisons at the cluster level $p < 0.05$ (FDR-corrected). Afterwards, FC values for each subject were extracted from the significant clusters of the ANOVA and post-hoc *t*-test analyses were conducted to identify differences between specific groups.

2.6. Network analysis of rs-fMRI

In addition to the seed-based FC approach, we investigated significant between-group differences in the whole-brain network connectivity (connectome) using the network-based statistic approach (NBS) (Zalesky et al., 2010).

NBS is a validated non-parametric method that has been used to control the family-wise error rate (FWER) when performing mass univariate testing on all connections in a network. NBS relies on the assumption that connectivity changes are more likely to affect multiples edges in a network (Fornito et al., 2016). Individual connectivity matrices were generated extracting the mean time series from 262 independent anatomical ROIs, which were defined based on the coordinates from an extensively validated parcellation system provided by (Power et al., 2011). Each ROI was modeled as a 10 mm diameter sphere with a minimum distance of 10 mm between sphere centers, thus avoiding potential overlapping. In addition, we discarded short-distance correlations less than 20 mm as they might be affected by spatial smoothing or reslicing. We focused only on positive correlations. The rationale of exploring between-group differences in the positive connectivity matrices was that it simplifies the interpretation of the results and allows us to have a better comprehension of our data. Thus, all links in the resulting NBS-component reflect differences in positive connectivity and are not a mixture of differences in negative and positive correlations. Here, a common mask was formed as the overlap of the averaged positive connectivity matrix of each group. NBS analysis was restricted to this common mask, which preserved 48% of connections. Components were identified using a primary component-forming threshold at $t > 3.5$. Permutation testing (10 000 permutations) was then applied to calculate FWE for every component previously identified. The final result controls FWER at $p < 0.05$.

For better illustration and representation, components were color-coded according to well-known resting-state networks (modules) (Bär et al., 2016). To compute these networks we used the graph theoretical approach. Firstly, an adjacency matrix (A_{ij}) was built by retaining 17% of the strongest connections of the average positive connectivity matrix. Secondly, A_{ij} was subsequently partitioned using the spectral approach based on the leading eigenvector of the modularity matrix (Bär et al., 2016; Newman, 2006). This graph partitioning led to four functionally distinct modules: the executive-control, the salience, the default mode network, and visual networks (see Supplementary Fig. S1). We used these networks as a reference to label the NBS components. NBS analysis was conducted using the Brain Connectivity Toolbox (Rubinov and Sporns, 2010), while graph partitioning and component visualization used in-house programs written in Python.

2.7. Simulation of aliasing effects

As stated, rs-fMRI data were sampled with a TR of 2.5 s, which means that the HR signal was aliased into the BOLD signal. Therefore, it is conceivable that the FC differences might be impacted by different

aliasing effects in the data.

To address this important issue, we simulated the effect of aliasing on the functional connectivity using different TRs and heart rates. We first generated time series of neuronal activity using vector autoregressive models (VAR) simulating Local Field Potentials (LFPs). Accumulating evidence suggests that LFPs response is a strong predictor of BOLD activity given the high correlation between LFPs and BOLD response (Logothetis et al., 2001). As LFPs generator, we used a slight variation of a simple VAR generative model defined by Roebroeck et al. (2005). Two interacting neuronal populations were generated as a realization of a bi-dimensional first-order VAR process with autoregression coefficients $A = \begin{bmatrix} 0.9 & 0 \\ 0.2 & 0.9 \end{bmatrix}$ and white noise with covariance matrix $\Sigma = \begin{bmatrix} 1 & 0 \\ 0 & 1 \end{bmatrix}$. We assumed a timestep of 2 ms (matching the physiological data recording frequency) and generated time series with a length of 650 s, from which we discarded the first 50 s prior to the analysis to allow the system to enter a steady state (Seth et al., 2013), thus simulating a standard rs-fMRI acquisition of 10 min. To generate simulated BOLD signals, the VAR model output was convolved with the canonical hemodynamic response function, which is derived from the difference between two gamma functions and has a temporal length of 25 seconds. We generated cardiac noise using sinusoidal waveforms with random phases at the fundamental frequency. Harmonics up to order two were subsequently added to the sinusoid to account for potential aliasing effects. However, since the amplitude of harmonics tend to decrease with the order of the harmonic (Cordes et al., 2001), the amplitude of the first and second harmonic were the half and the quarter of that of the fundamental frequency sinusoid. The resulting sinusoid was then converted into a non-stationary signal after adding a fifth-order polynomial trend (Nitzan et al., 1998) with random coefficients. This trend explicitly accounts for the effect of very slow non-periodic variations in the PPG signal due to some physiological or emotional activity (Nitzan et al., 1994). The presence of non-stationarity was confirmed by the Augmented Dickey-Fuller test ($p < 0.05$). Since the specific amount of physiological cardiac noise is not clear due to the variability reported in previous publications (Bianciardi et al., 2009b; Dagli et al., 1999; Shmueli et al., 2007), we defined the amount of cardiac pulsations to be the dominant source of noise (40%). Subsequently, these finally created BOLD signal time series were sampled at three different values of TR: TR = 2.52 s to simulate fMRI signal acquisition in the present study; TR = 0.72 s to simulate data acquired in the Human Connectome Project; and TR = 0.1 s to simulate the absence of aliasing. After sampling the time series, additional white Gaussian noise (20%) was added to mimic measurement error and noise in the acquisition (Roebroeck et al., 2005). Finally, BOLD signals were passband filtered into the resting-state band (0.01–0.1 Hz) and the FC was estimated. We set the "true" FC to 0.3 because we intended to examine the effect of aliasing on the hypothesized significant (i.e. significantly different from 0) functional connectivity between CAN regions. We repeated this procedure by varying the frequency of the PPG signal over the range of 40 bpm and 120 bpm in steps of 1 bpm.

3. Results

3.1. Physiological and demographic data

As summarized in Table 1, no significant differences were found between all HR groups with regard to age, gender and skin conductance measurements (SF and SCL). Physiological data that differed highly significantly between the groups were: HR, RMSSD (root mean square of the successive differences), LF/HF (ratio of low to high frequency of HR variability) and respiratory sinus arrhythmia. Further demographic and physiological data are listed in Table 1.

3.2. Main effects of group: differences in functional connectivity

Between-group functional connectivity differences (overall F-test) from the seed regions: right amygdala, right aI and VMPFC are depicted in Table 2 and Fig. 1. Analogous results from the seed regions of the left hemisphere are illustrated in Supplementary Fig. S2. For the right amygdala, significant overall FC differences were mainly located in areas reported to be involved in cardiac autonomic and emotional regulation, i.e. amygdala, aI and posterior insula (pI), left ventrolateral prefrontal cortex (VLPFC), ACC, periaqueductal gray area (PAG) and the dorsal vagal complex (DVC). Further clusters include the supplementary motor area (SMA), the hypothalamus and the cerebellum.

Table 1
Demographic and physiological data.

Parameter	SHR	MHR	FHR	p value[a]
Number of participants (n)	28	28	28	
Sex (m/f)	16/12	9/19	16/12	n.s.(0.1[b])
Age, mean (SD) [years]	31.14(10.43)	32.11(10.83)	31.50(11.00)	n.s(0.95)
Heart Rate, mean (SD) [bpm]	54.74(3.93)	66.87(3.71)	81.21(6.21)	4.4×10^{-33}
Respiratory Rate, mean (SD) [brpm]	15.71(2.80)	16.84(2.97)	15.75(4.02)	n.s.(0.37)
RMSSD, mean (SD) [ms]	73.86(29.06)	47.36(20.81)	34.08(16.14)	3.0×10^{-8}
LF/HF	1.09(0.47)	1.45(1.13)	2.61(2.70)	4.1×10^{-3}
Respiratory Sinus Arrhythmia [ms]	112.01(50.74)	82.94(42.53)	71.16(38.65)	3.4×10^{-3}
Self-rated Frequency of Physical Exercise[c] (n)	3-4 times per week (26)	1-2 times per week (11)	1-2 times per week (27)	n.s.(0.37[†])
SF [min^{-1}]	15.64(21.60)	23.18(24.17)	25.93(25.50)	n.s.(0.26)
SCL [μS]	0.88(0.76)	0.62(0.38)	0.95(0.95)	n.s.(0.24)

SD = standard deviation; bpm = beat-per-minute; brpm = breaths-per-minute; RMSSD = root mean squared of successive difference; ms = miliseconds; LF/HR = ratio of low to high frequency power of heart rate variability; SF = spontaneous fluctuations; SCL = level of skin conductance.

[a] p values resulting from one-way ANOVA F-test.

[b] p values resulting from $\chi 2$ test.

[c] Value in parentheses indicates the number of subjects reporting data.

With the right aI used as seed region, differences in the FC to the left and right amygdala, left and right pI, hypothalamus and cerebellum were observed. In addition, a cortical cluster showing different connectivity with the right aI was found in VMPFC. With respect to VMPFC-FC, overall between-group differences were detected for connectivity to the left aI as well as to the left and right VLPFC (Fig. 1 and Table 2).

We selected regions for the post-hoc *t*-test presented in Fig. 1 known to be involved in heart rate regulation. Post-hoc t-tests analyses (Fig. 1, side bars) revealed significantly ($p < 0.001$) increased connectivity of the right amygdala with left insula (the cluster included anterior and posterior insula) in the SHR group as compared to groups exhibiting higher HR. Moreover, the SHR group showed different behavior in hypothalamus and DVC regions; the opposed connectivity with respect to the other groups might reflect different neurophysiological mechanisms occurring uniquely at lower HR. On the other hand, increased negative connectivity was observed between VMPFC with left VLPFC and aI in groups with elevated HR. In total, we compared twenty clusters and in only two of them the functional connectivity was significantly lower in the slow HR group.

FC values in all analyzed clusters did not significantly differ between the MHR and FHR groups (Fig. 1, side bars).

We repeated these analyses using a parameter of HRV (RMSSD) as a covariate in the between-group analyses and observed similar results (Supplementary Fig. S4). Thus, it seems that significant between-group

Table 2
Main effect of Group.

Functional Connectivity to:	Right/Left	Brodmann's Area	Cluster size[a]	MNI coordinate			F value
				x	y	z	
Seed: Right Amygdala							
Inferior Frontal Gyrus	L	22/38/47	523	−54	16	−4	23,98
Superior Temporal Gyrus	L	22		−60	8	0	13,22
Insula	R	13	285	50	4	−6	14,07
Insula	L	13	365	−44	4	−4	14,56
Superior Temporal Gyrus	L	38		−44	6	−16	12,15
Amygdala	R	34	347	22	2	−18	19,91
Parahippocampal Gyrus	R	34		14	−12	−20	12,94
Superior Temporal Gyrus	R	38		24	10	−24	11,46
Hypothalamus	L		207	−4	−4	−14	15,31
Amygdala	L	34		−12	−6	−20	14,33
Parahippocampal Gyrus	L	36	95	−20	−34	−8	13,82
Parahippocampal Gyrus	R	36	587	20	−28	−8	28,65
Caudate Nucleus	R			30	−34	0	22,08
Anterior Cingulate Gyrus		24	106	0	38	10	10,51
Supplementary Motor Area		6	62	0	8	72	10,1
Middle Temporal Gyrus	R	39	*226*	50	−66	28	18,52
Dorsal Vagal Complex	L/R		638	4	−30	−52	25,26
PAG			101	2	−22	−8	13,53
Culmen	L		145	−4	−50	−18	16,43
Cerebellar Lingual	R			2	−44	−20	10,52
Seed: Left Amygdala							
Dorsolateral Prefrontal Cortex	L	10	88	−34	44	20	12,18
Inferior Frontal Gyrus	L	47	1600	−46	28	−4	24,22
Superior Temporal Gyrus	L	22/38		−50	0	−6	20,39
Insula	R	13	719	40	2	8	17,76
Amygdala	R	28		26	6	−24	15,03
Insula	R	13	44	36	16	−2	11,83
Parahippocampal Gyrus	R	34	66	18	−12	−18	16,74
Amygdala	R	34		18	0	−16	8,63
Parahippocampal Gyrus	R	36	252	20	−30	−8	25,02
Anterior Cingulate Gyrus	R	24	51	2	22	20	9,8
Precuneus	L	7	191	−24	−76	40	15,11
Precuneus	R	39	159	34	−66	36	11,28
Supplementary Motor Area		6	96	2	−24	74	12,44
Middle Temporal Gyrus	R	38	71	40	6	−38	8,25
Dorsal Vagal Complex			101	4	−38	−60	11,07
PAG/Red Nucleus			50	2	−26	−12	8,56
Culmen			111	−8	−34	−32	15,42
Seed: Right Anterior Insula							
Ventromedial Prefrontal Cortex	L	11	44	−10	42	−24	11,08
Ventrolateral Prefrontal Cortex	L	47	51	−42	30	0	12,41
Insula	R	13	249	38	−4	8	12,89
Insula	L	13/41	189	−38	−24	12	16,8
Amygdala	L		133	−24	−2	−22	13,19
Parahippocampal Gyrus	R	36	153	28	−24	−16	12,38
Parahippocampal Gyrus	R	34	77	18	−8	−22	11,03
Hypothalamus	L/R		72	2	2	−14	13,14
Posterior Cingulate/Precuneus	R	23	469	10	−56	20	16,96
Precuneus		23		0	−62	18	14,16
Dorsal Vagal Complex			329	−2	−24	−50	25,89
Declive			102	−2	−58	−18	11,31
Seed: Left Anterior Insula							
Ventromedial Prefrontal Cortex		11	205	0	28	−14	12,5
Inferior Frontal Gyrus	R	47	244	22	14	−20	13,23
Insula	R	13	385	36	−12	18	16,55
Amygdala	L	34	373	−18	−6	−20	16,39
Parahippocampal Gyrus	L	28		−18	−14	−22	12,38
Parahippocampal Gyrus	R	27	225	24	−32	−8	14,43
Hypothalamus			40	0	4	−12	10,74
Posterior Cingulate	R	23	129	10	−56	20	13,60
Superior Temporal Gyrus	L	22	642	−54	−10	6	16,47
Primary Motor Cortex	L	4		−60	−10	16	12,47
Dorsal Vagal Complex			270	4	−28	−52	19,06
Declive			71	−4	−56	−18	11,89
Seed: VMPFC							
Ventrolateral Prefrontal Cortex	R	38/44	130	56	12	0	12,80
Ventrolateral Prefrontal Cortex	L	22/47	67	−54	12	−4	12,62
Inferior Frontal Gyrus	L	46	56	−46	44	0	12,5
Insula	L	13/41	59	−34	14	4	9,04

[a] Voxel level $p < 0.001$ uncorrected, cluster level $p < 0.05$ FDR corrected.

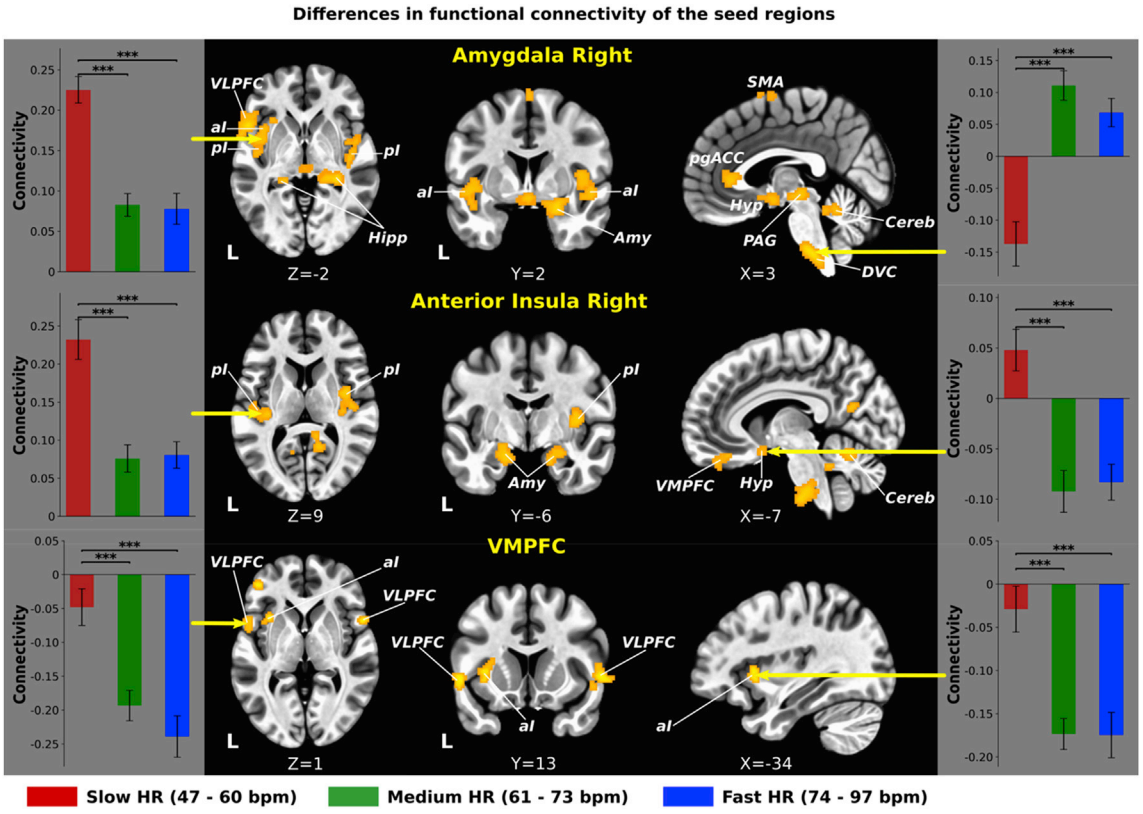

Fig. 1. Brain regions showing differences in functional connectivity using right amygdala, right anterior insula and VMPFC as seed regions, respectively. The F-test indicates a significant effect of HR at voxel level $p < 0.001$ and cluster level $p < 0.05$ (FDR-corrected). The bars depicted on the sides represent post-hoc t-tests carried out by averaging connectivity values on each significant cluster. Abbreviations: ***$p < 0.001$; VLPFC, ventrolateral prefrontal cortex; aI, anterior insula; pI, posterior insula; Hipp, hippocampus; Amy, amygdala; pgACC, pregenual ACC; Hyp, hypothalamus; SMA, supplementary motor area; Cereb, cerebellum; PAG, periaqueductal gray; DVC, dorsal vagal complex; SHR, slow heart rate group; MHR, medium heart rate group; FHR, fast heart rate group.

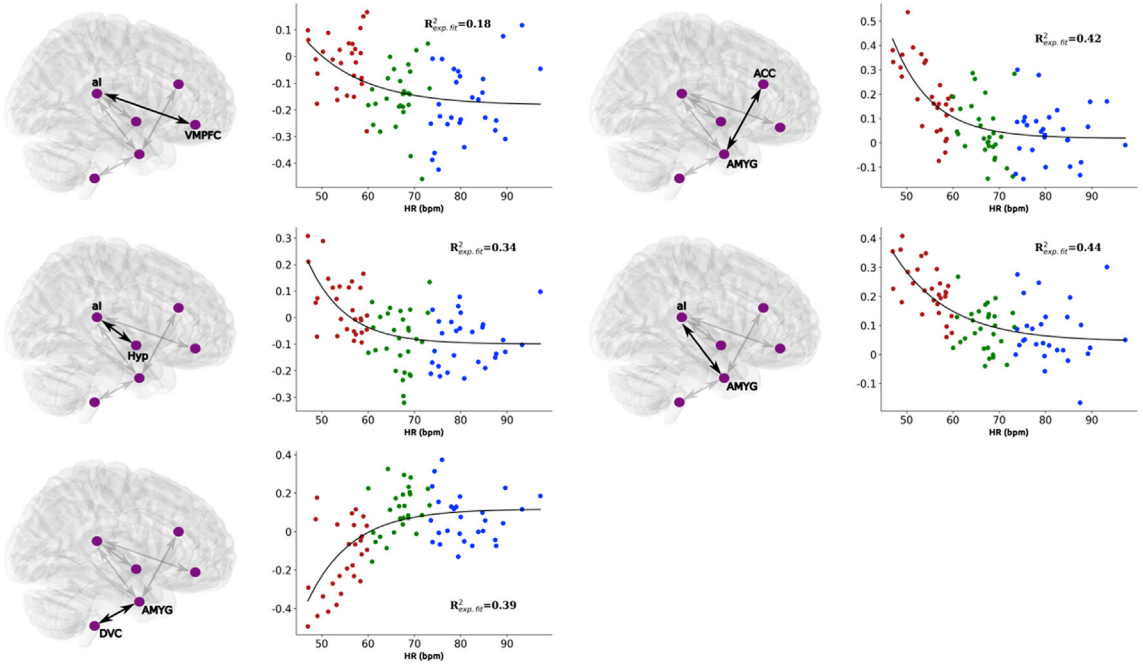

Fig. 2. Association between HR and functional connectivity of brain regions putatively involved in neurovisceral integration. Scatter plots refer to the connectivity indicated by the bold line with labels. Red points, SHR group; green points, MHR group; blue points, FHR group.

differences in HRV, in particular between SHR and FHR groups, have only a small effect on differences in functional connectivity of the CAN regions.

3.3. Relationship between HR and functional connectivity

To investigate the association between FC and HR within single HR-groups and across all subjects, regression analyses were performed with FC between specific CAN regions and heart rate.

Significantly negative associations between HR and FC was found in right amygdala-ACC ($r = -0.71$, $p < 0.001$), left aI-right amygdala ($r = -0.63$, $p < 0.001$), right aI-hypothalamus ($r = -0.53$, $p < 0.01$) and a significantly positive association between HR and right amygdala-DVC FC ($r = 0.46$, $p < 0.05$) in the SHR group.

The correlation between HR and FC was close to zero in the MHR and FHR groups. A different behavior was observed between VMPFC-left aI and right amygdala-DVC connectivities. In the former, the correlation was significantly positive ($r = 0.38$, $p < 0.05$) in the FHR and non-significant for SHR and MHR groups, while in the latter both SHR and MHR showed significant positive correlation with $r = 0.46$ ($p < 0.05$) and $r = 0.39$ ($p < 0.05$), respectively.

Furthermore, as illustrated in Fig. 2 it seems that the relationship between FC and HR becomes non-significant with increasing HR. Indeed, when we tested this observation, a non-linear exponential relationship explaining considerable variance between these variables was found when all subjects were analyzed together.

3.4. Network based statistics

With the NBS analysis, significantly greater positive functional connectivity was observed in the SHR as compared to the FHR group in a network of 35 nodes and 47 edges (Fig. 3: $p = 0.004$). Nodes within this network were located in CAN regions, i.e. amygdala, insula, ACC, but also in visual, temporal and sensorimotor regions with a large number of intra-hemispheric functional connections. Based on the modularity obtained by the spectral partition algorithm, 25 out 35 nodes were labeled as belonging to the salience network, 7 as belonging to the visual, 2 as belonging the default mode network (DMN) and 1 as belonging to the executive-control (Bär et al., 2016). Supplementary Table S1 contains a complete listing of nodes position and labels.

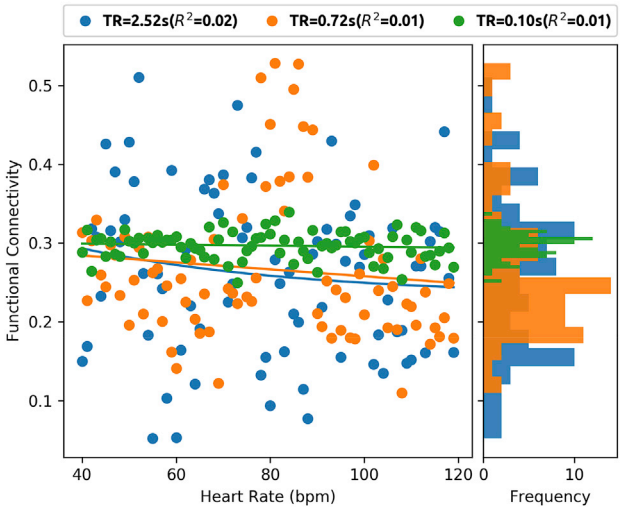

Fig. 4. Effect of simulated cardiac aliasing on functional connectivity for a wide range of heart rates and different sampling intervals (TR). R^2 values in parentheses indicate the variance explained by the exponential function used to approximate the FC values across the entire HR range. The side plot shows the FC histograms at the respective TR.

3.5. Simulation of aliasing effects on the FC

Fig. 4 illustrates FC values relative to HR extracted from simulated BOLD signal time series. A strong variability in the FC values was observed for the TR of 2.52 s, but without a significant linear or non-linear relationship between FC and HR. In the case of the fast TR of 0.72 s, as used in the Human Connectome Project, the variability in FC values was relatively small and the aliased HRs were easily detectable as FC peaks. It should be noted that HR higher than the sampling rate does not necessarily implies that its fundamental frequency aliases into the investigated resting-state low-frequency band (0.01–0.1 Hz). As expected in the absence of aliasing, i.e. TR = 0.1 s, FC remains stable across the entire HR range corresponding to the "true" correlation of 0.3. The histograms show the association between HR and FC depending on the three different sampling rates (TRs).

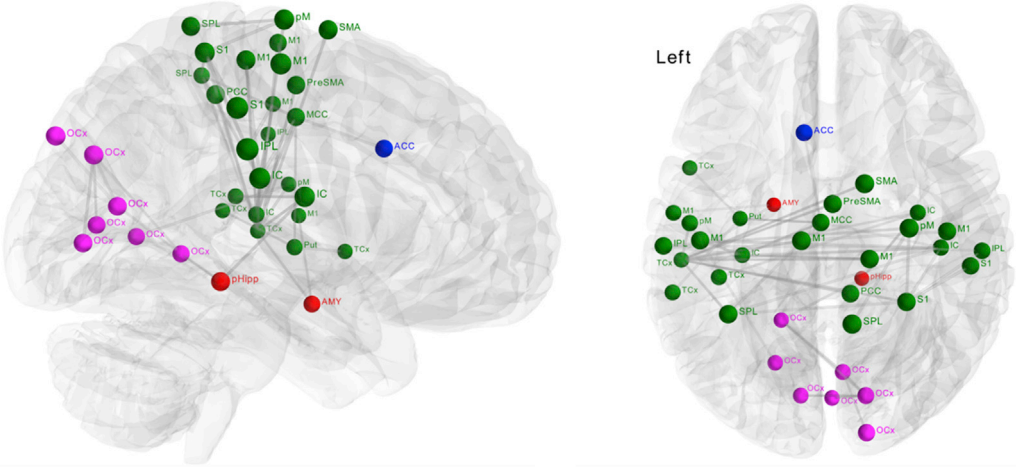

Fig. 3. Group comparisons (SHR vs FHR) in functional connectivity matrices using Network-Based statistics (NBS). The depicted component shows nodes with significantly ($p = 0.004$) higher connectivity in the SHR compared to FHR. These connections formed a single connected network with 35 nodes and 47 links. Colors indicate the resting-state network where the node belongs to, according to a community structure obtained using the spectral partition algorithm (Newman, 2006). Magenta, visual network; green, salience-network; red, default mode network; blue, executive-control network (see Supplementary Table S2 for abbreviations).

4. Discussion

The investigation of brain regions involved in cardiac regulation is an important issue in neuroscience research with respect to healthy aging or variety of medical conditions. Here we examined differences in RSFC within structures of the CAN between groups of healthy subjects classified according to their heart rate during the scanning procedure. To the best of our knowledge, this is the first study which systematically investigates changes in FC in relation to the mean heart rate. We focused on three brain regions of interest - the amygdala, the aI and the VMPFC - all belonging to the CAN and playing a prominent role within the framework of the Neurovisceral Integration Model (Thayer and Lane, 2000).

In agreement with our hypothesis, we found significant differences in the FC of these three ROIs, which were particularly noticeable between the groups with slow (<60 bmp) and fast HR (>75 bpm). Subjects with slow HR exhibited significantly increased FC between amygdala, insula, VLPFC, ACC, hippocampus and hypothalamus compared to subjects with medium or fast HR. In contrast, the groups with medium and fast HR mainly showed a FC close to zero.

The correlation analysis revealed a significant negative relationship between FC of regions within the CAN and HR, mainly in the SHR. Across all subjects, the relation between FC and HR could be described by a non-linear (exponential) course, i.e. with increasing heart rates the values of the functional connectivity in the CAN became lower - an observation that could be approximated by said non-linear relation.

The NBS analysis, supporting the results of the ROI analyses, revealed significantly stronger FC in the SHR group compared to the FHR group in a component comprising CAN regions including amygdala, insula, ACC and hippocampus, and additionally sensorimotor and occipital brain areas. Thus, we confirmed our hypothesis that the functional coupling of regions putatively involved in autonomic control is HR-dependent.

Previous studies consistently demonstrated that cardiac changes induced by short sessions of physical effort (Norton et al., 2013; Shoemaker et al., 2015; Williamson et al., 2003) elicit FC changes in CAN regions (Norton et al., 2013; Shoemaker et al., 2015). Norton and colleagues reported that during a simple handgrip task, activation in VMPFC and hippocampus was negatively correlated with changes in HR (Norton et al., 2013). Using effective connectivity, they also found that VMPFC exerts direct influence on the hippocampus and nuclei of the brainstem, which supports the notion of a top-down control by the VMPFC.

Slow HR is frequently found in meditation practitioners. In these subjects, a slowing in heart rate has been associated to structural changes within the cardiorespiratory centers as well as to increased connectivity between lower brainstem regions and cortical areas (Luders et al., 2011; Streeter et al., 2012; Vestergaard-Poulsen et al., 2009). In general, interventions using meditation techniques have been linked to increased parasympathetic activity, lower heart rate and stronger functional connectivity between CAN regions, in particular PCC, ACC, VMPFC and insula (Brewer et al., 2011; Kilpatrick et al., 2011; Streeter et al., 2012; Tang et al., 2012). Hypnosis is a similarly effective method to decrease HR (Barber and Hahn, 1963; Bauer and McCanne, 1980); putatively by shifting the sympathovagal balance toward an enhanced parasympathetic activity (Debenedittis et al., 1994). This is additionally accompanied by changes in the FC within CAN structures, such as increased FC between ACC with prefrontal cortex, insula and brainstem (Faymonville et al., 2003) as well as between DLPFC and insula (Jiang et al., 2017).

Although we did not explicitly manipulate the heart rate in the present study, we observed significant FC changes in regions reported in the above studies, which support our interpretation of an association between changes in FC within CAN regions and changes in heart rate.

Furthermore, slower HR is often found in individuals with regular physical activities and is a sign of healthy cardiovascular regulation (Blomqvist and Saltin, 1983; Scheuer and Tipton, 1977). However, we did not find any significant differences in the amount of self-rated physical activities between the groups (see Table 1). Therefore, we assume that a different degree of physical capacity is not a major influencing factor. In addition, we cannot explain differences in FC between groups by different levels of physiological arousal, because they were not significantly different with respect to skin conductance parameters (Armel and Ramachandran, 2003; Bach et al., 2010).

Several further factors can influence FC at rest (Finn et al., 2017). For instance, content and frequency of spontaneous thoughts (Christoff et al., 2009; Gorgolewski et al., 2014), mood (Harrison et al., 2008) and the kind of task performed before scanning (Barnes et al., 2009; Tung et al., 2013) might cause differences in FC. However, it seems unlikely that these factors cause such widespread and systematic FC changes (Laumann et al., 2015) as detected in the present study. Age is another important factor that might lead to changes in functional connectivity (Kumral et al., 2018; Sakaki et al., 2016) and heart rate (Boettger et al., 2010). In a recent study, Kumral et al. (2018) reported a strong association between resting HR variability (HRV) and FC in different age groups of healthy adults. Notably, a network including VMPFC, DLPFC, SMA, and cerebellum appeared to be HRV-dependent in younger adults (Kumral et al., 2018). Since our participants were all young adults and the groups did not significantly differ in age, it is unlikely that the effect of age may explain the observed differences in FC.

Another potentially relevant factor might be the degree of wakefulness in the resting state condition with closed eyes. In a typical resting state protocol, about one third of participants cannot maintain wakefulness and fall asleep (Tagliazucchi and Laufs, 2014). This percentage becomes even higher if subjects are instructed to keep their eyes closed (Tagliazucchi and Laufs, 2014), as in the present study. The wakefulness-sleep transition has been found to be also associated with fMRI signal changes (Chang et al., 2016; Laumann et al., 2017; Tagliazucchi et al., 2012; Tagliazucchi and Laufs, 2014) as well as with changes in physiological parameters like blood pressure and HR (Smith et al., 1998). As mentioned above, we did not find any differences in the level of physiological arousal as assessed by the skin conductance indices, which might be an indicator for changes in the degree of wakefulness (Sano et al., 2014).

One should also consider the possibility that the observed differences in the FC are due to different aliasing effects in the groups with slow and fast HR. To account for such potential effects on RSFC, we simulated the effect of aliasing on two BOLD signals sample with three different TR values. Based on our results of the simulation analysis, the observed between-group FC differences as well as the highly significant correlations between FC and HR in the SHR group seems not to be strongly affected by aliasing effects. As shown in the simulation, the FC shows a rather chaotic pattern when physiological cardiac noise dominates. Moreover, the fact that the coupling between FC and HR across all groups varied in an exponential manner (see Fig. 2) speaks against a global factor, such as aliasing, being the sole factor influencing the FC.

The applied state-of-the-art noise correction strengthens the assumption that our main findings cannot be solely explained by the differential effect of physiological cardiac noise on functional connectivities. The influence of these artifacts on the FC was controlled during the pre-processing steps through the RETROICOR approach, RVT and removal of low-frequency cardiac noise. The latter procedure was improved in the present study by using a HR-specific CRF, thus accounting for the varying effect of the cardiac rate on the shape of the CRF, which can lead to artificial group differences (de la Cruz et al., 2017). It should be noted that there is still an ongoing debate on how much physiological signal can be truly considered as “noise” (Iacovella and Hasson, 2011). A recent study showed that physiological noise correction methods particularly reduce fluctuations in regions known to be involved in cardiac autonomic regulation like insular cortices, brainstem and prefrontal areas (Khalili-Mahani et al., 2013). For example, by applying the full RETROICOR model and thus additionally removing the cardiac RETROICOR regressors, we observed that cluster sizes in the dorsal vagal center, hypothalamus and perigenual anterior cingulate cortex were reduced and did not reach the critical voxel size to pass the cluster-level

corrected statistical threshold (see Supplementary Fig. S3). The closeness of these clusters to ventricles make them particularly susceptible to physiological artifacts, which are therefore much stronger affected during physiological noise correction than other regions.

Finally, with regard to the NBS analysis, we detected in the SHR group a significantly stronger connected network than in the group with fast HR. This confirms the results of the ROI analyses and presumably reflects the neural basis of different cardiac autonomic balance. This network component also included several sensorimotor and visual regions. Studies with animals have found direct anatomical connections from sensorimotor cortex to parasympathetic nuclei in the lower brainstem, i.e. nucleus tractus solitarius and ventrolateral medulla (M'hamed et al., 1993; Verberne and Owens, 1998). In addition, the role of the sensorimotor cortex in autonomic control has been recognized in previous studies (Cechetto and Saper, 1990). Based on anatomical studies we can speculate that changes in the connectivity of sensorimotor areas are related to changes in the heart rate (Clancy et al., 2014; Sequeira and Ba-M'hamed, 1999; Viltart et al., 2003). In the case of the visual cortex, little is known about its relation to cardiac autonomic regulation and factors such as the state of wakefulness (Laumann et al., 2017; Tagliazucchi et al., 2012; Tagliazucchi and Laufs, 2014) or opening the eyes during scanning (Bianciardi et al., 2009a; Marx et al., 2004) might lead to FC alterations in these regions. Thus, further studies are required to systematically investigate the relationship between visual cortex connectivity and cardiac autonomic balance.

4.1. Implication for fMRI studies

Taken together, our results suggest that the variability in the RSFC is associated with inter-individual variability of the heart rate. If this finding is further corroborated in future studies, important implications for neuroimaging studies can be anticipated. We recommend to simultaneously assess HR in future fMRI studies to account for between- and within-groups differences. This is especially the case when comparing healthy subjects to patients with psychiatric disorders, which often exhibit significantly altered HR compared to control subjects (Bär, 2015; Schumann et al., 2017).

Furthermore, given the established link between HR and emotional, cognitive and social processes, present findings may also be considered to explain individual differences in brain activation or connectivity when using corresponding paradigms in the MR scanner to investigate such processes. Since the interaction between heart and brain are bidirectionally the present findings of significant brain-heart interaction may thus provide an interesting opportunity for further studies to relate functional connectivity in the cortico-subcortical circuitry to physiological responses as assessed by HR and to emotional/behavioral responses.

Present findings may also have implications for the better understanding of the neurovisceral integration model. This model is a framework to link psychological processes like emotion or cognition and the underlying cortico-subcortical neural circuit to cardiac autonomic regulation. Even if we used resting-state fMRI in the present study and thus did not investigate affective/cognitive processes, present findings indicate in support of the neurovisceral integration model a significant relationship between connectivity in the cortico-subcortical circuit and heart rate regulation. The observation of higher functional connectivity associated with lower heart rate indicates that slow oscillations in heart rate seem to strengthen brain network connectivity in this circuitry and potentially thereby exerting a positive effect on emotion regulation and self-control (Mather and Thayer, 2018). However, this relationship should be explicitly investigated in future studies.

4.2. Limitations

In this study, we used HR as the main parameter and did not use other physiological parameters, such as HRV metrics. The decision to use HR was motivated by the fact that it is influenced by both sympathetic and parasympathetic modulation and that HRV metrics are more prone to errors in signal recording than HR and can be corrupted by respiratory effects (Hill and Siebenbrock, 2009; Penttilä et al., 2001).

We are aware that HR also covariates with the physiological cardiac noise in the BOLD signal, which implies, for example, that the FC in regions likely affected by pulsation should also correlate with HR. However, these artifacts should represent only a small portion of the resting-state signal (de Munck et al., 2008) and as indicated earlier, its potential influence was minimized by applying state-of-the-art physiological noise correction techniques.

Furthermore, as recently demonstrated in rodents (Kim et al., 2016), local changes in cerebral blood flow and pressure can also impact resting firing activity of neurons, the so-called vasculo-neuronal coupling (VNC), potentially having an effect on FC. However, we consider that gross fluctuations in vascular variables are properly accounted for during the physiological correction steps.

To obtain fMRI data free of aliasing, a TR below 0.3 seconds or even shorter is necessary, which is currently challenging with respect to the whole-brain acquisition. To simulate aliasing effects, we used a model to estimate its impact on the association between different HRs and low-frequency BOLD fluctuations, which indicated that the relationship between HR and FC is unlikely to be dominated by aliasing. However, we did not explicitly model heart rate variability (HRV), but instead we introduced non-stationarity into the model by adding a fifth-order polynomial trend to the simulated data. Heart rate variability comprises frequencies that may contribute to the fMRI frequency spectrum and may additionally influence the functional connectivity. Modeling HRV requires varying the beat-to-beat distances within a range of physiologically plausible values and also accounting for other physiological variables like respiration, which was beyond the scope of this work. But, we used HRV (RMSSD) as covariate and observed similar results as in the original analyses (Supplementary Fig. S4). Future studies with sufficiently short TR should replicate present findings, where aliasing effects do not play a major role.

5. Conclusion

Our study represents the first direct demonstration of the relation between heart rate and functional connectivity of brain regions in the CAN. The functional coupling between these regions becomes stronger when the heart rate is lower. Furthermore, we showed that this relationship is non-linear and can be approximated by an exponential function. Using synthetic fMRI and cardiac data, we demonstrated that aliasing cannot explain our findings. Future investigations should examine the relationship between functional connectivity and heart rate measured with sufficiently short TR.

Acknowledgement

This work was supported by the German Research Council (DFG grant FI BA 3848/9-1)

Appendix A. Supplementary data

Supplementary data to this article can be found online at https://doi.org/10.1016/j.neuroimage.2019.04.014.

References

Armel, K.C., Ramachandran, V.S., 2003. Projecting sensations to external objects: evidence from skin conductance response. Proc. R. Soc. B Biol. Sci. 270, 1499–1506. https://doi.org/10.1098/rspb.2003.2364.

Bach, D.R., Friston, K.J., Dolan, R.J., 2010. Analytic measures for quantification of arousal from spontaneous skin conductance fluctuations. Int. J. Psychophysiol. 76, 52–55. https://doi.org/10.1016/j.ijpsycho.2010.01.011.

Bär, K.-J., 2015. Cardiac autonomic dysfunction in patients with schizophrenia and their healthy relatives – a small review. Front. Neurol. 6, 139. https://doi.org/10.3389/fneur.2015.00139.

Bär, K.J., De la Cruz, F., Schumann, A., Koehler, S., Sauer, H., Critchley, H., Wagner, G., 2016. Functional connectivity and network analysis of midbrain and brainstem nuclei. Neuroimage 134, 53–63. https://doi.org/10.1016/j.neuroimage.2016.03.071.

Barber, T.X., Hahn, K.W., 1963. Hypnotic induction and "Relaxation." Arch. Gen. Psychiatr. 8, 295. https://doi.org/10.1001/archpsyc.1963.01720090083010.

Barnes, A., Bullmore, E.T., Suckling, J., 2009. Endogenous human brain dynamics recover slowly following cognitive effort. PLoS One 4 e6626. https://doi.org/10.1371/journal.pone.0006626.

Bauer, K.E., McCanne, T.R., 1980. Autonomic and central nervous system responding: during hypnosis and simulation of hypnosis. Int. J. Clin. Exp. Hypn. 28, 148–163. https://doi.org/10.1080/00207148008409837.

Beissner, F., Meissner, K., Bär, K.-J., Napadow, V., 2013. The autonomic brain: an activation likelihood estimation meta-analysis for central processing of autonomic function. J. Neurosci. 33, 10503–10511. https://doi.org/10.1523/JNEUROSCI.1103-13.2013.

Benarroch, E.E., 1993. The central autonomic network: functional organization, dysfunction, and perspective. Mayo Clin. Proc. 68, 988–1001.

Bhattacharyya, P.K., Lowe, M.J., 2004. Cardiac-induced physiologic noise in tissue is a direct observation of cardiac-induced fluctuations. Magn. Reson. Imaging 22, 9–13. https://doi.org/10.1016/j.mri.2003.08.003.

Bianciardi, M., Fukunaga, M., van Gelderen, P., Horovitz, S.G., de Zwart, J.A., Duyn, J.H., 2009a. Modulation of spontaneous fMRI activity in human visual cortex by behavioral state. Neuroimage 45, 160–168. https://doi.org/10.1016/j.neuroimage.2008.10.034.

Bianciardi, M., Fukunaga, M., van Gelderen, P., Horovitz, S.G., de Zwart, J.A., Shmueli, K., Duyn, J.H., 2009b. Sources of functional magnetic resonance imaging signal fluctuations in the human brain at rest: a 7 T study. Magn. Reson. Imaging 27, 1019–1029. https://doi.org/10.1016/j.mri.2009.02.004.

Birn, R.M., Diamond, J.B., Smith, M.A., Bandettini, P.A., 2006. Separating respiratory-variation-related fluctuations from neuronal-activity-related fluctuations in fMRI. Neuroimage 31, 1536–1548. https://doi.org/10.1016/j.neuroimage.2006.02.048.

Birn, R.M., Murphy, K., Bandettini, P.A., 2008. The effect of respiration variations on independent component analysis results of resting state functional connectivity. Hum. Brain Mapp. 29, 740–750. https://doi.org/10.1002/hbm.20577 (The).

Biswal, B., Yetkin, F.Z., Haughton, V.M., Hyde, J.S., 1995. Functional connectivity in the motor cortex of resting human brain using echo-planar MRI. Magn. Reson. Med. 34, 537–541.

Blomqvist, C.G., Saltin, B., 1983. Cardiovascular adaptations to physical training. Annu. Rev. Physiol. 45, 169–189. https://doi.org/10.1146/annurev.ph.45.030183.001125.

Boettger, M.K., Schulz, S., Berger, S., Tancer, M., Yeragani, V.K., Voss, A., Bär, K.-J., 2010. Influence of age on linear and nonlinear measures of autonomic cardiovascular modulation. Ann. Noninvasive Electrocardiol. 15, 165–174. https://doi.org/10.1111/j.1542-474X.2010.00358.x.

Boucsein, W., 1992. Electrodermal Activity. Plenum Press.

Brewer, J.A., Worhunsky, P.D., Gray, J.R., Tang, Y.-Y., Weber, J., Kober, H., 2011. Meditation experience is associated with differences in default mode network activity and connectivity. Proc. Natl. Acad. Sci. Unit. States Am. 108, 20254–20259. https://doi.org/10.1073/pnas.1112029108.

Bright, M.G., Murphy, K., 2015. Is fMRI "noise" really noise? Resting state nuisance regressors remove variance with network structure. Neuroimage 114, 158–169. https://doi.org/10.1016/j.neuroimage.2015.03.070.

Buckner, R.L., Andrews-Hanna, J.R., Schacter, D.L., 2008. The brain's default network. Ann. N. Y. Acad. Sci. 1124, 1–38. https://doi.org/10.1196/annals.1440.011.

Cauda, F., Costa, T., Torta, D.M.E., Sacco, K., D'Agata, F., Duca, S., Geminiani, G., Fox, P.T., Vercelli, A., 2012. Meta-analytic clustering of the insular cortex. Characterizing the meta-analytic connectivity of the insula when involved in active tasks. Neuroimage 62, 343–355. https://doi.org/10.1016/j.neuroimage.2012.04.012.

Cauda, F., D'Agata, F., Sacco, K., Duca, S., Geminiani, G., Vercelli, A., 2011. Functional connectivity of the insula in the resting brain. Neuroimage 55, 8–23. https://doi.org/10.1016/j.neuroimage.2010.11.049.

Cechetto, D., Saper, C., 1990. Role of the cerebral cortex in autonomic function. In: Loewy, A., Spyer, K. (Eds.), Central Regulation of Autonomic Functions. Oxford University Press, Oxford, UK, pp. 208–223.

Chang, C., Cunningham, J.P., Glover, G.H., 2009. Influence of heart rate on the BOLD signal: the cardiac response function. Neuroimage 44, 857–869. https://doi.org/10.1016/j.neuroimage.2008.09.029.

Chang, C., Leopold, D.A., Schölvinck, M.L., Mandelkow, H., Picchioni, D., Liu, X., Ye, F.Q., Turchi, J.N., Duyn, J.H., 2016. Tracking brain arousal fluctuations with fMRI. Proc. Natl. Acad. Sci. Unit. States Am. 113 (16), 4518–4523. https://doi.org/10.1073/pnas.1520613113.

Chang, C., Metzger, C.D., Glover, G.H., Duyn, J.H., Heinze, H.-J., Walter, M., 2013. Association between heart rate variability and fluctuations in resting-state functional connectivity. Neuroimage 68, 93–104. https://doi.org/10.1016/j.neuroimage.2012.11.038.

Christoff, K., Gordon, A.M., Smallwood, J., Smith, R., Schooler, J.W., 2009. Experience sampling during fMRI reveals default network and executive system contributions to mind wandering. Proc. Natl. Acad. Sci. U. S. A 106, 8719–8724. https://doi.org/10.1073/pnas.0900234106.

Clancy, J.A., Johnson, R., Raw, R., Deuchars, S.A., Deuchars, J., 2014. Anodal transcranial direct current stimulation (tDCS) over the motor cortex increases sympathetic nerve activity. Brain Stimul 7, 97–104. https://doi.org/10.1016/J.BRS.2013.08.005.

Cordes, D., Haughton, V.M., Arfanakis, K., Carew, J.D., Turski, P.A., Moritz, C.H., Quigley, M.A., Meyerand, Elizabeth, M, Vmh, R., Elizabeth Meyerand, M., 2001. Frequencies contributing to functional connectivity in the cerebral cortex in "'Resting-state'" data. AJNR Am J Neuroradiol From Dep. Med. Phys. 22, 1326–1333.

Dagli, M.S., Ingeholm, J.E., Haxby, J.V., 1999. Localization of cardiac-induced signal change in fMRI. Neuroimage 9, 407–415. https://doi.org/10.1006/nimg.1998.0424.

de la Cruz, F., Schumann, A., Koehler, S., Bär, K.-J., Wagner, G., Köhler, S., Bär, K.-J., Wagner, G., 2017. Impact of the heart rate on the shape of the cardiac response function. Neuroimage 162, 214–225. https://doi.org/10.1016/j.neuroimage.2017.08.076.

de Munck, J.C.C., Gonçalves, S.I.I., Faes, T.J.C.J.C., Kuijer, J.P.A.P.A., Pouwels, P.J.W.J.W., Heethaar, R.M.M., Lopes da Silva, F.H.H., 2008. A study of the brain's resting state based on alpha band power, heart rate and fMRI. Neuroimage 42, 112–121. https://doi.org/10.1016/j.neuroimage.2008.04.244.

Debenedittis, G., Cigada, M., Bianchi, A., Signorini, M.G., Cerutti, S., 1994. Autonomic changes during hypnosis: a heart rate variability power spectrum analysis as a marker of sympatho-vagal balance. Int. J. Clin. Exp. Hypn. 42, 140–152. https://doi.org/10.1080/00207149408409347.

Deco, G., Hagmann, P., Hudetz, A.G., Tononi, G., 2014. Modeling resting-state functional networks when the cortex falls asleep: local and global changes. Cereb. Cortex 24, 3180–3194. https://doi.org/10.1093/cercor/bht176.

Faymonville, M.-E., Roediger, L., Del Fiore, G., Delgueldre, C., Phillips, C., Lamy, M., Luxen, A., Maquet, P., Laureys, S., 2003. Increased cerebral functional connectivity underlying the antinociceptive effects of hypnosis. Cogn. Brain Res. 17, 255–262. https://doi.org/10.1016/S0926-6410(03)00113-7.

Finn, E.S., Scheinost, D., Finn, D.M., Shen, X., Papademetris, X., Constable, R.T., 2017. Can brain state be manipulated to emphasize individual differences in functional connectivity? Neuroimage 160, 140–151. https://doi.org/10.1016/j.neuroimage.2017.03.064.

Fornito, A., Zalesky, A., Bullmore, E.T., 2016. Fundamentals of Brain Network Analysis. https://doi.org/10.1016/C2012-0-06036-X.

Glover, G.H., Li, T.Q., Ress, D., 2000. Image-based method for retrospective correction of physiological motion effects in fMRI: RETROICOR. Magn. Reson. Med. 44, 162–167.

Gorgolewski, K.J., Lurie, D., Urchs, S., Kipping, J.A., Craddock, R.C., Milham, M.P., Margulies, D.S., Smallwood, J., 2014. A correspondence between individual differences in the brain's intrinsic functional architecture and the content and form of self-generated thoughts. PLoS One 9 e97176. https://doi.org/10.1371/journal.pone.0097176.

Greicius, M.D., Krasnow, B., Reiss, A.L., Menon, V., 2003. Functional connectivity in the resting brain: a network analysis of the default mode hypothesis. Proc. Natl. Acad. Sci. U. S. A 100, 253–258. https://doi.org/10.1073/pnas.0135058100.

Harrison, B.J., Pujol, J., Ortiz, H., Fornito, A., Pantelis, C., Yücel, M., 2008. Modulation of brain resting-state networks by sad mood induction. PLoS One 3 e1794. https://doi.org/10.1371/journal.pone.0001794.

Hill, L.K., Siebenbrock, A., 2009. Are all measures created equal? Heart rate variability and respiration - biomed 2009. Biomed. Sci. Instrum. 45, 71–76.

Iacovella, V., Hasson, U., 2011. The relationship between BOLD signal and autonomic nervous system functions: implications for processing of "physiological noise". Magn. Reson. Imaging 29, 1338–1345. https://doi.org/10.1016/j.mri.2011.03.006.

Iglesias, J.E., Liu, Cheng-Yi, Thompson, P.M., Tu, Zhuowen, 2011. Robust brain extraction across datasets and comparison with publicly available methods. IEEE Trans. Med. Imaging 30, 1617–1634. https://doi.org/10.1109/TMI.2011.2138152.

Jiang, H., White, M.P., Greicius, M.D., Waelde, L.C., Spiegel, D., 2017. Brain activity and functional connectivity associated with hypnosis. Cereb. Cortex 27 (8), 4083–4093. https://doi.org/10.1093/cercor/bhw220.

Jo, H.J., Saad, Z.S., Simmons, W.K., Milbury, L.A., Cox, R.W., 2010. Mapping sources of correlation in resting state FMRI, with artifact detection and removal. Neuroimage 52, 571–582. https://doi.org/10.1016/j.neuroimage.2010.04.246.

Khalili-Mahani, N., Chang, C., van Osch, M.J., Veer, I.M., van Buchem, M.A., Dahan, A., Beckmann, C.F., van Gerven, J.M.A., Rombouts, S.A.R.B., 2013. The impact of "physiological correction" on functional connectivity analysis of pharmacological resting state fMRI. Neuroimage 65, 499–510. https://doi.org/10.1016/j.neuroimage.2012.09.044.

Kilpatrick, L.A., Suyenobu, B.Y., Smith, S.R., Bueller, J.A., Goodman, T., Creswell, J.D., Tillisch, K., Mayer, E.A., Naliboff, B.D., 2011. Impact of Mindfulness-Based Stress Reduction training on intrinsic brain connectivity. Neuroimage 56, 290–298. https://doi.org/10.1016/j.neuroimage.2011.02.034.

Kim, K.J., Ramiro Diaz, J., Iddings, J.A., Filosa, J.A., 2016. Vasculo-neuronal coupling: retrograde vascular communication to brain neurons. J. Neurosci. 36, 12624–12639. https://doi.org/10.1523/JNEUROSCI.1300-16.2016.

Kumral, D., Schaare, H.L., Beyer, F., Reinelt, J., Uhlig, M., Liem, F., Lampe, L., Babayan, A., Reiter, A., Erbey, M., Roebbig, J., Loeffler, M., Schroeter, M.L., Husser, D., Witte, A.V., Villringer, A., Gaebler, M., 2018. The age-dependent relationship between resting heart rate variability and functional brain connectivity. Neuroimage 185, 521–533. https://doi.org/10.1016/J.NEUROIMAGE.2018.10.027.

Laumann, T.O., Gordon, E.M., Adeyemo, B., Snyder, A.Z., Joo, S.J., Chen, M.Y., Gilmore, A.W., McDermott, K.B., Nelson, S.M., Dosenbach, N.U.F., Schlaggar, B.L., Mumford, J.A., Poldrack, R.A., Petersen, S.E., 2015. Functional system and areal organization of a highly sampled individual human brain. Neuron 87 (3), 657–670. https://doi.org/10.1016/j.neuron.2015.06.037.

Laumann, T.O., Snyder, A.Z., Mitra, A., Gordon, E.M., Gratton, C., Adeyemo, B., Gilmore, A.W., Nelson, S.M., Berg, J.J., Greene, D.J., McCarthy, J.E., Tagliazucchi, E., Laufs, H., Schlaggar, B.L., Dosenbach, N.U.F., Petersen, S.E., 2017. On the stability of BOLD fMRI correlations. Cereb. Cortex 27 (10), 4719–4732. https://doi.org/10.1093/cercor/bhw265.

Lim, C.L., Rennie, C., Barry, R.J., Bahramali, H., Lazzaro, I., Manor, B., Gordon, E., 1997. Decomposing skin conductance into tonic and phasic components. Int. J. Psychophysiol. 25, 97–109.

Logothetis, N.K., Pauls, J., Augath, M., Trinath, T., Oeltermann, A., 2001. Neurophysiological investigation of the basis of the fMRI signal. Nature 412, 150–157. https://doi.org/10.1038/35084005.

Lowe, M.J., 1999. Gram-schmidt orthogonalization to reduce aliased physiologic noise in low sampling rate f'MR1 data. In: Proc ISMRM 7th Annu. Meet. Philadelphia, p. 1711.

Luders, E., Clark, K., Narr, K.L., Toga, A.W., 2011. Enhanced brain connectivity in long-term meditation practitioners. Neuroimage 57, 1308–1316. https://doi.org/10.1016/j.neuroimage.2011.05.075.

Lund, T.E., Madsen, K.H., Sidaros, K., Luo, W.-L., Nichols, T.E., 2006. Non-white noise in fMRI: does modelling have an impact? Neuroimage 29, 54–66. https://doi.org/10.1016/j.neuroimage.2005.07.005.

Mather, M., Thayer, J.F., 2018. How heart rate variability affects emotion regulation brain networks. Curr. Opin. Behav. Sci. 19, 98–104. https://doi.org/https://doi.org/10.1016/j.cobeha.2017.12.017.

M'hamed, S.B., Sequeira, H., Poulain, P., Bennis, M., Roy, J.C., 1993. Sensorimotor cortex projections to the ventrolateral and the dorsomedial medulla oblongata in the rat. Neurosci. Lett. 164, 195–198. https://doi.org/10.1016/0304-3940(93)90890-W.

Maldjian, J.A., Laurienti, P.J., Burdette, J.H., 2004. Precentral gyrus discrepancy in electronic versions of the Talairach atlas. Neuroimage 21, 450–455.

Maldjian, J.A., Laurienti, P.J., Kraft, R.A., Burdette, J.H., 2003. An automated method for neuroanatomic and cytoarchitectonic atlas-based interrogation of fMRI data sets. Neuroimage 19, 1233–1239.

Marx, E., Deutschländer, A., Stephan, T., Dieterich, M., Wiesmann, M., Brandt, T., 2004. Eyes open and eyes closed as rest conditions: impact on brain activation patterns. Neuroimage 21, 1818–1824. https://doi.org/10.1016/J.NEUROIMAGE.2003.12.026.

Menon, V., 2015. Salience network. In: Toga, A.W. (Ed.), Brain Mapping: an Encyclopedic Reference, vol. 2. Academic Press, Elsevier, pp. 597–611.

Newman, M.E.J., 2006. Modularity and community structure in networks. PNAS Proc. Natl. Acad. Sci. United States Am. 103, 8577–8582. https://doi.org/10.1073/pnas.0601602103.

Nitzan, M., Babchenko, A., Khanokh, B., Landau, D., 1998. The variability of the photoplethysmographic signal - a potential method for the evaluation of the autonomic nervous system. Physiol. Meas. 19, 93–102. https://doi.org/10.1088/0967-3334/19/1/008.

Nitzan, M., de Boer, H., Turivnenko, S., Babchenko, A., Sapoznikov, D., 1994. Power spectrum analysis of spontaneous fluctuations in the photoplethysmographic signal. J. Basic Clin. Physiol. Pharmacol. 5, 269–276. https://doi.org/10.1515/JBCPP.1994.5.3-4.269.

Norton, K.N., Luchyshyn, T.A., Kevin Shoemaker, J., 2013. Evidence for a medial prefrontal cortex–hippocampal axis associated with heart rate control in conscious humans. Brain Res. 1538, 104–115. https://doi.org/10.1016/j.brainres.2013.09.032.

Patterson, J.C., Ungerleider, L.G., Bandettini, P.A., 2002. Task-independent functional brain activity correlation with skin conductance changes: an fMRI study. Neuroimage 17, 1797–1806. https://doi.org/10.1006/NIMG.2002.1306.

Penttilä, J., Helminen, A., Jartti, T., Kuusela, T., Huikuri, H.V., Tulppo, M.P., Coffeng, R., Scheinin, H., 2001. Time domain, geometrical and frequency domain analysis of cardiac vagal outflow: effects of various respiratory patterns. Clin. Physiol. 21, 365–376.

Power, J.D., Cohen, A.L., Nelson, S.M., Wig, G.S., Barnes, K.A., Church, J.A., Vogel, A.C., Laumann, T.O., Miezin, F.M., Schlaggar, B.L., Petersen, S.E., 2011. Functional network organization of the human brain. Neuron 72, 665–678. https://doi.org/10.1016/j.neuron.2011.09.006.

Roebroeck, A., Formisano, E., Goebel, R., 2005. Mapping directed influence over the brain using Granger causality and fMRI. Neuroimage 25, 230–242. https://doi.org/10.1016/j.neuroimage.2004.11.017.

Rubinov, M., Sporns, O., 2010. Complex network measures of brain connectivity: uses and interpretations. Neuroimage 52, 1059–1069. https://doi.org/10.1016/j.neuroimage.2009.10.003.

Sakaki, M., Yoo, H.J., Nga, L., Lee, T.H., Thayer, J.F., Mather, M., 2016. Heart rate variability is associated with amygdala functional connectivity with MPFC across younger and older adults. Neuroimage 139, 44–52. https://doi.org/10.1016/j.neuroimage.2016.05.076.

Sano, A., Picard, R.W., Stickgold, R., 2014. Quantitative analysis of wrist electrodermal activity during sleep. Int. J. Psychophysiol. 94, 382–389. https://doi.org/10.1016/j.ijpsycho.2014.09.011.

Scheuer, J., Tipton, C.M., 1977. Cardiovascular adaptations to physical training. Annu. Rev. Physiol. 39, 221–251. https://doi.org/10.1146/annurev.ph.39.030177.001253.

Schumann, A., Andrack, C., Bär, K.-J., 2017. Differences of sympathetic and parasympathetic modulation in major depression. Prog. Neuro-Psychopharmacol. Biol. Psychiatry 79, 324–331. https://doi.org/10.1016/j.pnpbp.2017.07.009.

Sequeira, H., Ba-M'hamed, S., 1999. Pyramidal control of heart rate and arterial pressure in cats. Arch. Ital. Biol. 137, 47–62.

Seth, A.K., Chorley, P., Barnett, L.C., 2013. Granger causality analysis of fMRI BOLD signals is invariant to hemodynamic convolution but not downsampling. Neuroimage 65, 540–555. https://doi.org/10.1016/j.neuroimage.2012.09.049.

Shmueli, K., van Gelderen, P., de Zwart, J.A., Horovitz, S.G., Fukunaga, M., Jansma, J.M., Duyn, J.H., 2007. Low-frequency fluctuations in the cardiac rate as a source of variance in the resting-state fMRI BOLD signal. Neuroimage 38, 306–320. https://doi.org/10.1016/j.neuroimage.2007.07.037.

Shoemaker, J.K., Norton, K.N., Baker, J., Luchyshyn, T., 2015. Forebrain organization for autonomic cardiovascular control. Auton. Neurosci. Basic Clin. 188, 5–9. https://doi.org/10.1016/j.autneu.2014.10.022.

Smith, R.P., Veale, D., Pépin, J.-L., Lévy, P.A., 1998. Obstructive sleep apnoea and the autonomic nervous system. Sleep Med. Rev. 2, 69–92. https://doi.org/10.1016/S1087-0792(98)90001-6.

Streeter, C.C., Gerbarg, P.L., Saper, R.B., Ciraulo, D.A., Brown, R.P., 2012. Effects of yoga on the autonomic nervous system, gamma-aminobutyric-acid, and allostasis in epilepsy, depression, and post-traumatic stress disorder. Med. Hypotheses 78, 571–579.

Tagliazucchi, E., Laufs, H., 2014. Decoding wakefulness levels from typical fMRI resting-state data reveals reliable drifts between wakefulness and sleep. Neuron 82, 695–708. https://doi.org/10.1016/J.NEURON.2014.03.020.

Tagliazucchi, E., von Wegner, F., Morzelewski, A., Borisov, S., Jahnke, K., Laufs, H., 2012. Automatic sleep staging using fMRI functional connectivity data. Neuroimage 63, 63–72. https://doi.org/10.1016/J.NEUROIMAGE.2012.06.036.

Tang, Y.Y., Rothbart, M.K., Posner, M.I., 2012. Neural correlates of establishing, maintaining, and switching brain states. Trends Cognit. Sci. 16, 330–337. https://doi.org/10.1016/j.tics.2012.05.001.

Thayer, J.F., Åhs, F., Fredrikson, M., Sollers, J.J., Wager, T.D., 2012. A meta-analysis of heart rate variability and neuroimaging studies: implications for heart rate variability as a marker of stress and health. Neurosci. Biobehav. Rev. 36, 747–756. https://doi.org/10.1016/j.neubiorev.2011.11.009.

Thayer, J.F., Lane, R.D., 2009. Claude Bernard and the heart-brain connection: further elaboration of a model of neurovisceral integration. Neurosci. Biobehav. Rev. 33 (2), 81–88. https://doi.org/10.1016/j.neubiorev.2008.08.004.

Thayer, J.F., Lane, R.D., 2000. A model of neurovisceral integration in emotion regulation and dysregulation. J. Affect. Disord. 61, 201–216. https://doi.org/10.1016/S0165-0327(00)00338-4.

Tong, Y., Lindsey, K.P., Frederick, B.D., 2011. Partitioning of physiological noise signals in the brain with concurrent near-infrared spectroscopy and fMRI. J. Cereb. Blood Flow Metab. 31, 2352–2362. https://doi.org/10.1038/jcbfm.2011.100.

Tung, K.-C., Uh, J., Mao, D., Xu, F., Xiao, G., Lu, H., 2013. Alterations in resting functional connectivity due to recent motor task. Neuroimage 78, 316–324. https://doi.org/10.1016/J.NEUROIMAGE.2013.04.006.

Verberne, A.J., Owens, N.C., 1998. Cortical modulation of theCardiovascular system. Prog. Neurobiol. 54, 149–168. https://doi.org/10.1016/S0301-0082(97)00056-7.

Vestergaard-Poulsen, P., Van Beek, M., Skewes, J., Bjarkam, C.R., Stubberup, M., Bertelsen, J., Roepstorff, A., 2009. Long-term meditation is associated with increased gray matter density in the brain stem. Neuroreport 20, 170–174. https://doi.org/10.1097/WNR.0b013e328320012a.

Viltart, O., Mullier, O., Bernet, F., Poulain, P., Ba-M'Hamed, S., Sequeira, H., 2003. Motor cortical control of cardiovascular bulbar neurones projecting to spinal autonomic areas. J. Neurosci. Res. 73, 122–135. https://doi.org/10.1002/jnr.10598.

Williamson, J.W., McColl, R., Mathews, D., 2003. Evidence for central command activation of the human insular cortex during exercise. J. Appl. Physiol. 94, 1726–1734. https://doi.org/10.1152/japplphysiol.01152.2002.

Zalesky, A., Fornito, A., Bullmore, E.T., 2010. Network-based statistic: identifying differences in brain networks. Neuroimage 53, 1197–1207. https://doi.org/10.1016/j.neuroimage.2010.06.041.

Zar, J.H., 1996. Biostatistical Analysis. Prentice-Hall international editions (Prentice Hall).